Chemical Engineering Journal 150 (2009) 536–543

Contents lists available at ScienceDirect

Chemical Engineering Journal

journal homepage: www.elsevier.com/locate/cej

Experimental study of reactive mixing in a mini-scale mixer by laser-induced fluorescence technique

Zhe Liu, Yi Cheng*, Yong Jin

Department of Chemical Engineering, Tsinghua University, Beijing 100084, PR China

ARTICLE INFO

Article history:
Received 21 November 2008
Received in revised form 22 March 2009
Accepted 23 March 2009

Keywords:
Mixing
Reactive mixing
Reactive-LIF
Measurement technique
Mini-reactor

ABSTRACT

The liquid–liquid mixing process coupled with chemical reactions in a mini-scale jet mixer was visualized by reactive laser-induced fluorescence (reactive-LIF) technique for a deep understanding of the interplay between the mixing and the simultaneous reactions. A novel approach for implementing the reactive-LIF measurements was advanced in this work, where the principle was based on the quenching of the fluorescence signal emitted from the Rhodamine-B dye using the mechanism of Fenton reaction. The purely physical mixing and the reactive mixing processes were investigated extensively by comparing the concentration fields under different operating conditions, i.e. the different momentum ratios between the jet and the bulk flows, and the different Reynolds numbers in the mixing channel of a mini-scale mixer. The results revealed that the transient dynamics in the reactive mixing process cannot be precisely understood based on the time-averaged concentration fields from either the physical or the reactive mixing measurements. The coupled mixing and the reaction processes occurred simultaneously, unless the rapid mixing was achieved by tuning the operating conditions so that the processes can be decoupled into two isolated ones.

1. Introduction

As a principal process mixing usually has a significant effect on the performance of chemical reactors [1], because chemical reactions always occur together with the process of different reactive materials contacting each other. The relationship between mixing and reactions depends on the relative magnitude of the mixing time scale and the reaction time scale. If the former is much smaller than the latter, the reactions could be considered to start after a well-mixed state, and the perfect mixing models such as the CSTR model might be adequate. However, when the former is similar with or bigger than the latter, the mixing efficiency could greatly alter the system performances such as the reaction selectivity and the products distribution, especially in the processes where the side reactions produce undesired by-products [2,3]. Therefore, control of the mixing process is often the key technology in process engineering for a wide class of products [4]. The interaction of turbulent mixing and fast chemical reactions has been investigated in depth by a few research groups. For example, a series of articles by the group of Fox [5–10] have made unique contributions in this area. They applied particle image velocimetry (PIV) and laser-induced fluorescence (LIF) technique to reveal the simultaneous velocity and concentration fields in the turbulent mixing process, and advanced several simulation methods based on the micro-mixing models. The group of Bourne [11–13] investigated mixing and chemical reactions by experiments and discussed the interaction between reactions and mixing on various scales. Although great efforts have been made on this topic, there is still a demand for a deeper understanding on the reactive mixing.

The experimental approaches to study the mixing performance could be classified into two categories: the one by test reactions, and the other by visualization techniques.

The test reactions have been summarized into three main types, i.e. the single reaction ($A + B \rightarrow R$), the consecutive competing reactions ($A + B \rightarrow R$ and $R + B \rightarrow S$), and the parallel competing reactions ($A + B \rightarrow R$ and $C + B \rightarrow S$) [14]. In the latter two schemes, yield and/or selectivity achieved for the specific reaction products can be used to quantify the mixing performance. Lots of researches were carried out by this means, such as the "Villermaux/Dushmann method" [15–19], and the "third Bourne" reactions [3,20–21]. Although the micro-mixing efficiency can be evaluated in various mixers, only the integral mixing effect is obtained by these methods because only the products at the mixer outlets are analyzed. That is to say the micro-mixing efficiency is evaluated indirectly by using the test reactions.

Laser-induced fluorescence (LIF) technique has been frequently employed for mixing research in the past few years in both macro- and micro-sized devices [8,22–27], which is a non-intrusive

* Corresponding author. Tel.: +86 10 6279 4468; fax: +86 10 6277 2051.
E-mail address: yicheng@tsinghua.edu.cn (Y. Cheng).

1385-8947/$ – see front matter © 2009 Elsevier B.V. All rights reserved.
doi:10.1016/j.cej.2009.03.041

Nomenclature

$\bar{C}$	normalized concentration of species B at the complete mixing positions
C_B	normalized concentration of species B
$C_{B,phy}$	normalized concentration of species B in the physical mixing experiments
$C_{B,react}$	normalized concentration of species B in the reactive mixing experiments
d	edge length of the cross-section of the mixing channel in x–z plane (mm)
Q_A	flow rate of fluid A (mL min^{-1})
Q_B	flow rate of fluid B (mL min^{-1})
x_i	local mixing rate at each interrogation area

Greek symbols

α	flow rate ratio of two fluids
Φ	mixing extent
η	reaction extent

approach to visualize the concentration (or temperature) field with high resolution in time and in space. The principle of the LIF technique is based on the monotonic relationship between the fluorescent tracer concentration and the excited fluorescence intensity by the laser sheet through the liquids. Therefore the concentration field in the mixing zone could be visualized quantitatively, showing the dynamic mixing process of liquid streams. The predominant advantage of LIF technique over the test reactions is that it could reveal the meso- or micro-scale mixing information at each point in the mixing zone. In our previous work [28–30], LIF technique was successfully employed to assess the mixing performance in several jet mixers for fast liquid mixing design. However, all these studies focused on the physical mixing process, which is not adequate for analyzing the potential reactive mixing process where chemical reactions occur in time.

Some researchers have implemented the LIF technique for reactive mixing measurement by using reaction-sensitive fluorescents instead of the ordinary LIF tracers. The measured fluorescence intensity changes with the development of the chemical reaction(s). Thus, the extent of the reaction procedure can be characterized by the spatial distribution of the dynamically changed species concentration in terms of the fluorescence variation. Ito and Komori [31] utilized 'Rhodamine-2' ($C_{40}H_{43}ClN_4O_{11}$) as the reactive-LIF tracer, for it does not emit fluorescence unless chelating with Ca^{2+} ion. Hence, the solutions with 'Rhodamine-2' and calcium chloride were used as the two reactive streams, respectively. Shinohara et al. [32] visualized reacting flows based on the pH-dependent fluorescence dye (i.e. 'quinine'), where the fluorescence intensity is correlated with the pH value of the solution. In their experiments, acetic acid solution and ammonia hydroxide solution were employed as the two reactive streams. Therefore a neutralization reaction took place together with the mixing process, and the reaction progress was revealed by the dynamic signals of the fluorescence intensity.

Although the reactive-LIF technique could visualize the competitive relationship between mixing and chemical reactions, the prices for the laser apparatus and the fluorescence tracer become the limiting factors for the reactive-LIF experiments. The specific tracer can only be excited by a laser with a certain wavelength, e.g. 'quinine' by 355 nm and 'Rhodamine-2' by 532 nm. These reaction-sensitive tracers usually bear a prohibitive price, for example, 'Rhodamine-2' for more than 200 dollars per milligram.

In this work, we advanced a novel approach to realize the reactive-LIF measurement in liquid phase based on an ordinary laser apparatus at 532 nm and the low price fluorescence tracer of Rhodamine-B. The reactive mixing process in a mini-scale jet mixer was measured and the relationship between the reaction and the mixing in the mixing zone were analyzed.

2. Experimental

2.1. Reactive-LIF technique

Different from a general LIF technique, reactive-LIF measurement must be able to capture the variation of a species concentration in time due to the joint effect of mixing and reaction. And it should be able to visualize and quantify the interplay between the physical mixing and the simultaneous chemical reactions. The basic idea of the proposed reactive-LIF technique is to use a reaction to quench the fluorescence signal, so that the reactive mixing process can be recorded quantitatively. In this approach, a fluorescence tracer is dissolved in one of the two streams to be mixed. When the two streams mix, the tracer concentration field, which also represents the species concentration from one stream, could be visualized due to the difference of the fluorescence intensity in the mixing zone. A chemical reaction for quenching the fluorescence signal is introduced by adding another liquid stream, which takes place simultaneously with the mixing process. With a certain consumption rate of the fluorescence tracer, this model reaction can be applied to mimic an interested kinetics to identify the effect of mixing on the reaction performance. To be noted, the reaction should be powerful enough to oxidize the tracer added in fluids for quenching the fluorescence signals. Among many oxidation reactions, the *Fenton reaction* was chosen for its effectiveness for a wide variety of organic substances. The kinetics and mechanism are discussed as follows.

Fenton reaction, named as its finder [33], reveals that the ferrous ion could strongly promote the hydrogen peroxide to oxidize the malic acid. Subsequent studies had shown that the combination of H_2O_2 and a ferrous salt, i.e. the Fenton's reagents, is an effective oxidant. The mechanism of the Fenton reaction was explained by Haber and Weiss [34] as a hydroxyl radical reaction, where the reaction of Fe^{2+} with H_2O_2 in an aqueous solution leads to the formation of a hydroxyl radical ($OH^\bullet$) (reaction (1)). Barb et al. [35] investigated further the mechanism of Fenton reaction and proposed a second-order kinetic model. The reaction rate constant of reaction (1) was reported on the magnitude of 10^2 L mol^{-1} s^{-1}. Once the $OH^\bullet$ is formed, it will rapidly oxidize the organic substance in the solution, including the fluorescence tracer, with a reaction rate constant of 10^7 to 10^{10} L mol^{-1} s^{-1} [36]. Although there exist some arguments on the mechanism of Fenton reaction [37], the approach can be well adopted in the reactive-LIF measurement. That is, when Rhodamine-B (absorption spectrum: 460–590 nm, max = 550 nm; emission spectrum 550–680 nm, max = 590 nm) is oxidized, the fluorescence signal will disappear. And, the model reaction to quench the fluorescence signals can be considered as a fast reaction with a reaction rate constant on the magnitude of 10^2 L mol^{-1} s^{-1}:

$$Fe^{2+} + H_2O_2 \rightarrow Fe^{3+} + HO^\bullet + HO^- \quad (1)$$

The novelty of the proposed reactive-LIF technique lies in the two aspects. Firstly, the inexpensive dye, i.e. Rhodamine-B, was employed in the measurements, instead of very expensive dyes such as Rhodamine-2 or Rhodamine-WT. As a result, LIF measurements on the liquid mixing processes with large flow rates can be feasible. Secondly, the reactive-LIF approach employed the oxidation reaction mechanism to make the fluorescence from Rhodamine-B quenched so that the reactive mixing process can be measured in time and in space. As a contrast, the principle of reactive-LIF experiments using Rhodamine-2 was based on the combination reaction, as described above.

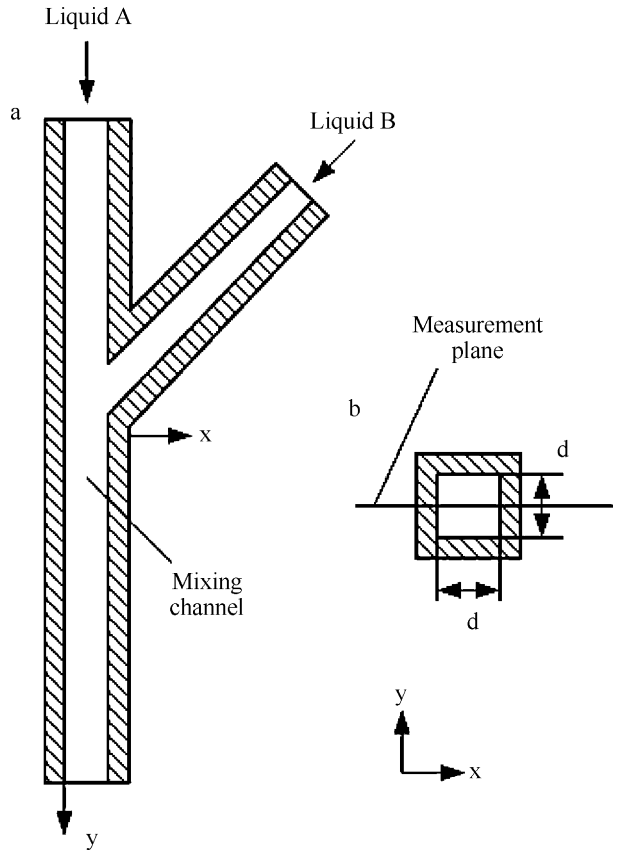

Fig. 1. Schematic of the mini-scale jet mixer.

2.2. Experimental procedure

In the reactive-LIF experiments, a mini-scale jet flow mixer shown in Fig. 1 was employed. The cross-section of the mixing channel in *x*–*z* plane was square with the edge length equivalent to 2 mm, i.e. $d = 2$ mm. The measurement plane was located in the center of *z* direction. Two liquid streams, named A and B, were confined into the small-size channels, respectively, and then impinged into each other at an angle of 45° in the mixing channel. The angle was arbitrarily chosen following our previous work [28].

Fig. 2 shows the schematic diagram of the reactive-LIF experimental system. Liquids A and B were pumped into the inlets of the jet mixer by two syringe pumps. A 1.5 W diode pumped solid-state continuous laser with the characteristic wavelength at 532 nm was used as the illumination source. The laser was transformed to a thin sheet, less than 1 mm in thickness, to lighten the measurement plane. The images of the lighted flow filed were captured by an 8-bit CCD camera with the image size of 1024 × 1080 pixels. The advantage of CCD camera is its higher sensitivity and less noise than a CMOS camera. The corresponding spatial resolution was 50 μm/pix. Thus, the flow behaviors in meso-mixing scale can be captured. A high-pass optical filter in front of the camera filtered the scattered and reflected laser to ensure that only the fluorescence was received by the camera. The FLOWMAP (Dantec Dynamics) software package was used for the data acquisition. The time interval between two adjacent pictures was 0.25 s, i.e. the time resolution equivalent to 4 frame/s.

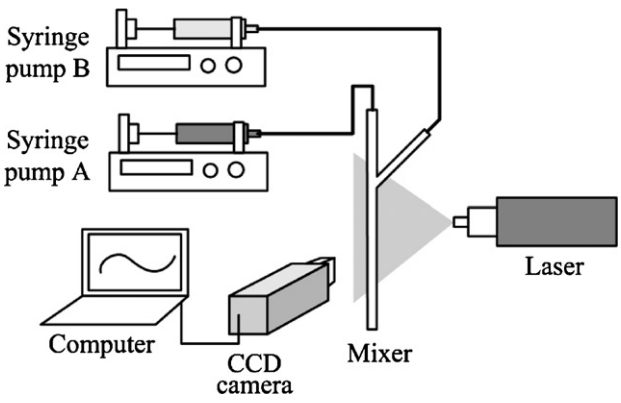

Fig. 2. Schematic diagram of the reactive-LIF experimental system.

The whole experiment process contained three series of sub-experiments, i.e. experiment-I, -II and -III, for system calibration, physical mixing measurement and reactive mixing measurement, respectively. For experiment-I, both liquids A and B were the Rhodamine-B aqueous solution with the same concentration. After fixing the relative positions of the laser, the mixer and the CCD camera, five different concentrations of Rhodamine-B aqueous solutions were used to flow through the mixing channel, i.e. 20, 40, 60, 80, and 100 μg/L, and the fluorescence signals were captured by the camera for *in situ* calibration.

For experiment-II, de-ionized water was acted as the liquid A, and the Rhodamine-B aqueous solution (100 μg/L) was used as the liquid B. Table 1 shows the operating conditions for the purely physical mixing measurements. Different momentum ratios between liquids A and B, and different Reynolds numbers in the mixing zone were investigated.

Experiment-III was based on experiment-II, that is, each case in experiment-III took the same flow conditions of experiment-II (see Table 1). However, the substances in liquids A and B were modified: H_2O_2 was added in the de-ionized water as the liquid A; Fe^{2+} was dissolved in the Rhodamine-B aqueous solution as the liquid B. Therefore, Fenton reaction would occur when the two streams contacted each other. As a result, the reactive mixing process is directly visualized by the LIF measurement in the experiment-III.

Under these flow conditions, the half-life of the mixing is estimated at 1.7–17 ms, and the residence time in the system is at the range of 10–100 ms. The half-life of the reaction, which is related to the chemical reaction rate constant, is about 10 ms. Thus, the reaction time scale can be smaller than the mixing time scale under some operating conditions.

3. Results and discussion

3.1. Concentration field in the mixing zone

Figs. 3 and 4 show the images by LIF measurements corresponding to some of the cases listed in Table 1. Colors in these images represent the normalized concentration of the fluorescent tracer, which also indicates the concentration of the liquid B, pure red denoting 100% concentration of the liquid B and the pure blue denoting 0%. In Fig. 3, the time-averaged concentration fields in the mixing zones of physical and reactive mixing cases are compared. Each time-averaged image is an average of 100 transient measurements, i.e. the average over 25 s.

Under the same flow conditions, purely physical mixing and reactive mixing exhibit different species distribution patterns in the mixing zones, as shown in the pair comparisons of Fig. 3-1a and 1b, 2-2a and 2b, 3-3a and 3b. For example, at the *y* position of 20 mm in Fig. 3-1a, a clear interface between streams A and B exists in the physical mixing process, where the concentration of liquid B on the right-hand side of this interface is almost homogenous maintaining more than 0.9. However, there exists a sub-flow with the low concentration about 0.7, stretching through at the same *y* position in the reacting mixing process (see Fig. 3-1b). Similarly,

Table 1
Operating conditions for experiment-II and -III.

Exp.-II case	Liquid A (bulk)	Liquid B (jet)	Momentum of liquid A	Momentum of liquid B	Momentum ratio (jet:bulk)	Re number in mixing zone	Exp.-III case	Liquid A (bulk)	Liquid B (jet)
Phy-1	Water	Rh-B 100 μg/L	1.88×10^{-4} kg m s^{-2}	3.76×10^{-4} kg m s^{-2}	1:2	1300	React-1	H_2O_2 7.5%	Rh-B 100 μg/L, Fe^{2+} 0.07 mol/L
Phy-2	Water	Rh-B 100 μg/L	4.44×10^{-4} kg m s^{-2}	8.88×10^{-4} kg m s^{-2}	1:2	2000	React-2	H_2O_2 7.5%	Rh-B 100 μg/L, Fe^{2+} 0.07 mol/L
Phy-3	Water	Rh-B 100 μg/L	8.10×10^{-4} kg m s^{-2}	16.2×10^{-4} kg m s^{-2}	1:2	2700	React-2	H_2O_2 7.5%	Rh-B 100 μg/L, Fe^{2+} 0.07 mol/L
Phy-4	Water	Rh-B 100 μg/L	4.23×10^{-4} kg m s^{-2}	4.23×10^{-4} kg m s^{-2}	1:1	1300	React-4	H_2O_2 7.5%	Rh-B 100 μg/L, Fe^{2+} 0.07 mol/L
Phy-5	Water	Rh-B 100 μg/L	10.0×10^{-4} kg m s^{-2}	10.0×10^{-4} kg m s^{-2}	1:1	2000	React-5	H_2O_2 7.5%	Rh-B 100 μg/L, Fe^{2+} 0.07 mol/L
Phy-6	Water	Rh-B 100 μg/L	18.2×10^{-4} kg m s^{-2}	18.2×10^{-4} kg m s^{-2}	1:1	2700	React-6	H_2O_2 7.5%	Rh-B 100 μg/L, Fe^{2+} 0.07 mol/L
Phy-7	Water	Rh-B 100 μg/L	3.76×10^{-4} kg m s^{-2}	1.88×10^{-4} kg m s^{-2}	2:1	1300	React-7	H_2O_2 7.5%	Rh-B 100 μg/L, Fe^{2+} 0.07 mol/L
Phy-8	Water	Rh-B 100 μg/L	8.88×10^{-4} kg m s^{-2}	4.44×10^{-4} kg m s^{-2}	2:1	2000	React-8	H_2O_2 7.5%	Rh-B 100 μg/L, Fe^{2+} 0.07 mol/L
Phy-9	Water	Rh-B 100 μg/L	16.2×10^{-4} kg m s^{-2}	8.10×10^{-4} kg m s^{-2}	2:1	2700	React-9	H_2O_2 7.5%	Rh-B 100 μg/L, Fe^{2+} 0.07 mol/L

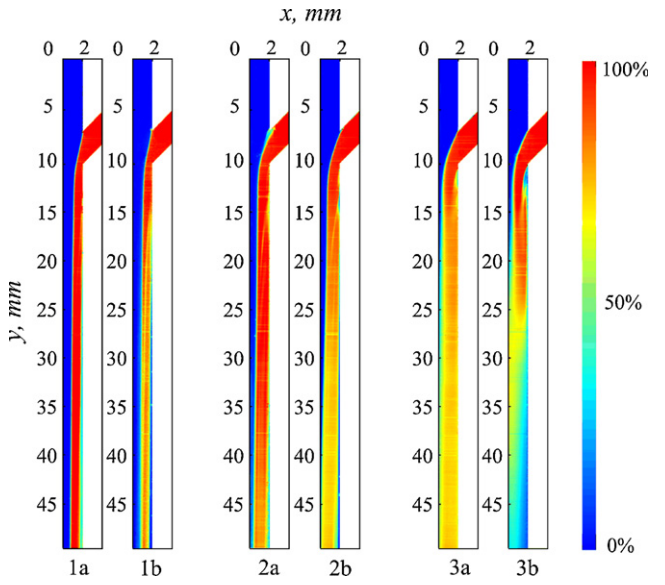

Fig. 3. Pseudo-color images of time-averaged concentration field: (1a) case Phy-1; (1b) case React-1; (2a) case Phy-4; (2b) case React-4; (3a) case Phy-7; (3b) case React-7.

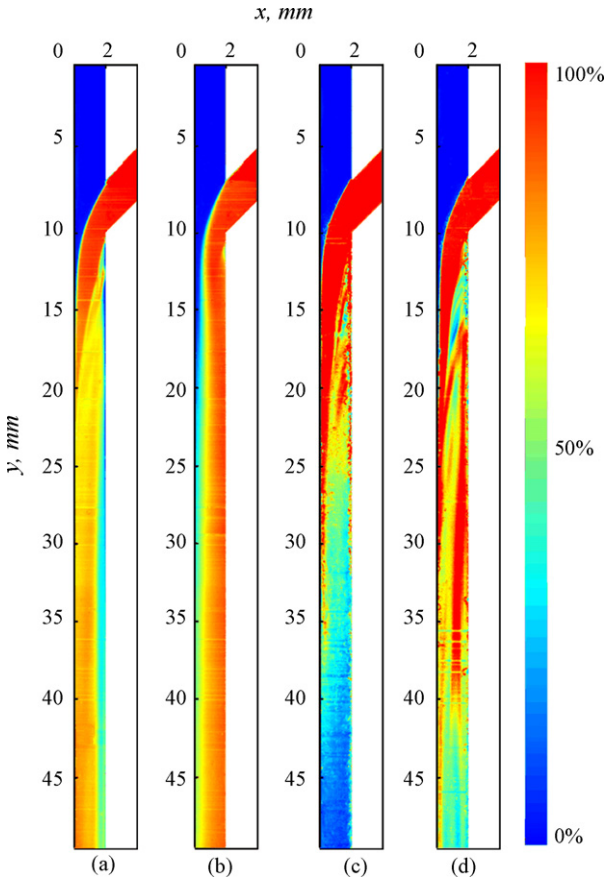

Fig. 4. LIF measurements of transient concentration field: (a and b) case Phy-7; (c and d) case React-7.

the high concentration of liquid B from the jet flow changes gradually to a relative low status along the y direction in Fig. 3-3a. But in Fig. 3-3b, the high concentration region jumps to a low concentration status due to the reaction process coupled with the physical mixing.

Fig. 4 shows the representative results of transient concentration fields of cases Phy-7 and React-7. Different from the time-averaged images in Fig. 3-3a and b, the transient phenomena in both physical and reactive mixing processes have clear random nature, especially that in the reactive mixing process the consumption of the reagents at each spatial point has nonlinear dependence on the local composition of the mixed fluid flow. In Fig. 4c and d, the significant difference of species distribution pattern in the mixing zone can be observed directly. The liquid B seems to be suddenly consumed after jetting into the bulk flow in Fig. 4c, which is almost consumed completely at the y position of 40 mm. But in Fig. 4d, the liquid B appears to be torn into several sub-flows, and about 40% of species B still exists at the bottom of the measurement zone, i.e. $y = 50$ mm. This indicates that the species fluctuation in the reactive mixing zone should be considered carefully when we intend to improve the selectivity to desired product(s) in a competing reaction system. The time-averaged results may miss lots of information in either physical or reactive mixing process, and the information on the purely physical mixing is not sufficient to help understand the reactive mixing process. Actually, the figures of transient concentration fields present the concentration distributions at different time intervals, which are the non-averaged concentration fields. Obviously, the camera used in our LIF experiments with a temporal resolution of 4 frames/s is not sufficient to analyze the periodic or turbulent fluctuations. Since there are not two transient results bearing exactly the same concentration distribution, several pictures are chosen arbitrarily for Fig. 4. The transient results can bring us an insight that there really exists significant difference between transient and time-averaged results, and this is the purpose to give Fig. 4. The transient results were observed at all Reynolds numbers in our experimental conditions, and the similar conclusions were obtained.

Fig. 5 plots more quantitative concentration information at different y positions for the cases compared in Fig. 3. The solid symbols indicate the normalized concentration of Rhodamine-B in the purely physical mixing cases, while the hollow symbols indicate that in the corresponding reactive mixing cases. The concentration lines for physical and reactive mixing in each pair of corresponding cases present similar relationships: these two lines firstly stretch at almost the same values when y is low, but the reactive line goes much lower than the physical one with the development of mixing process, i.e. at larger y values. To see the comparison of cases Phy-4 and React-4 in Fig. 4, for example, the physical mixing line and the reactive mixing line have almost the same value at the y positions of 10 and 15 mm. However at the downstream positions, a difference about 20% in value emerges between these two lines. Similar results also appear to the cases Phy-7 and React-7: at the y position of 45 mm, the concentration value is around 0.7 in the physical mixing, but about 0.3 in the reactive mixing. These differences are evidently caused by the underlying reactions which consume the reagent(s) in liquid B.

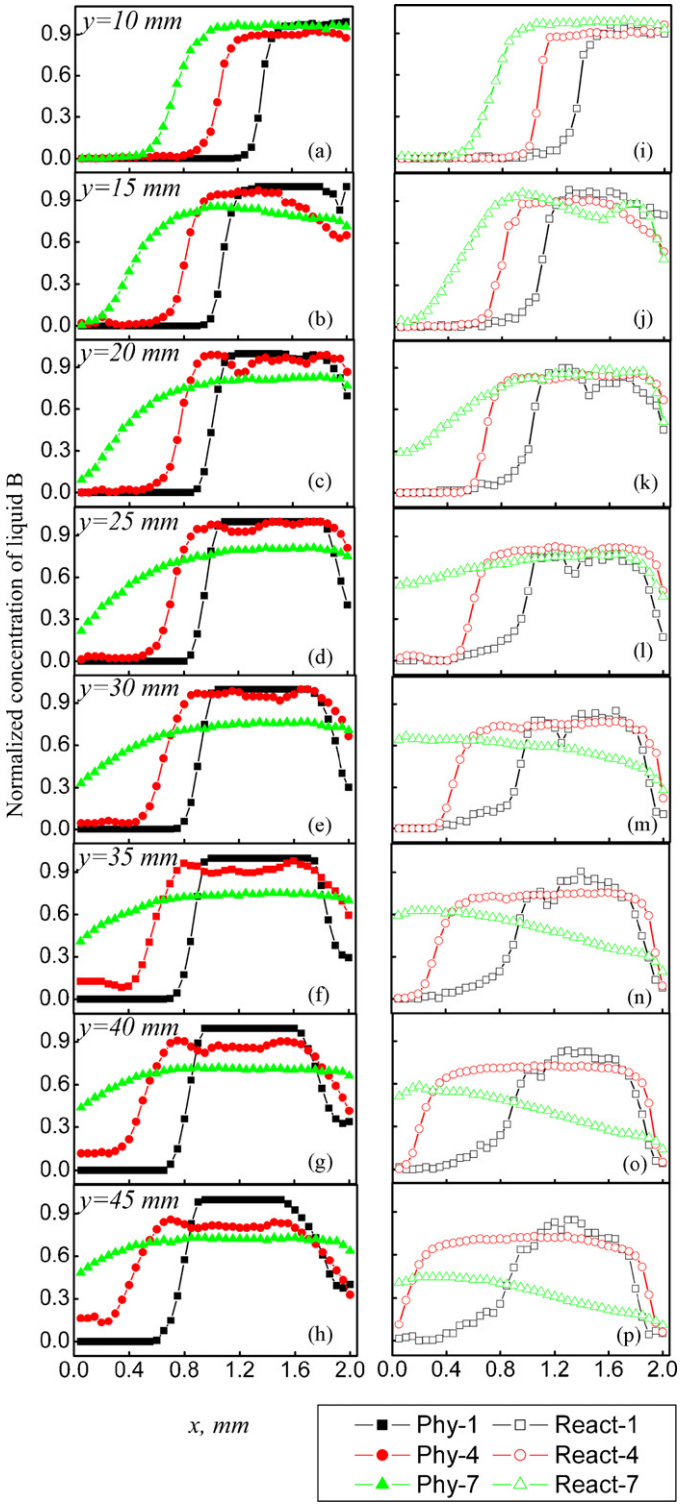

Fig. 5. Time-averaged concentration fields at different y positions for cases Phy-1, 4, 7 and cases React-1, 4, 7.

3.2. Relative extent of mixing and reaction

In order to assess the relationship between mixing and reaction quantitatively, two parameters are defined in this section to characterize the mixing and reaction extents, respectively.

3.2.1. Definition of mixing extent, Φ

To estimate the mixing extent, parameter Φ is defined according to the work of Ito and Komori [31]. When the flow rate ratio of two fluids, Q_B/Q_A, is equal to $1/\alpha$, the concentration of species B at the complete mixing, $\bar{C}$, is expressed as

$$\bar{C} = \frac{1}{1+\alpha} \tag{2}$$

Then the local mixing rate at each interrogation area, x_i, is defined as

$$x_i = \begin{cases} \dfrac{C_B}{\bar{C}} & (C_B \le \bar{C}) \\ \dfrac{1 - C_B}{1 - \bar{C}} & (C_B > \bar{C}) \end{cases} \quad (3)$$

where C_B is the normalized concentration of species from liquid B digitized by the LIF in physical mixing experiments, i.e. experiment-II.

This definition of x_i indicates that the two chemical species are homogeneously mixed when the complete mixing is accomplished. That is, the normalized concentrations of completely mixed non-reacting species A and B must be $1/(1+\alpha)$ and $\alpha/(1+\alpha)$ at all points at the cross-sectional area of the mixing channel, respectively. The mixing extent at the cross-section, Φ, is calculated by averaging x_i in the spanwise x direction. The parameter (L) is the width of the mixing channel:

$$\Phi = \frac{1}{L}\int_0^L x_i dx \quad (4)$$

Therefore the mixing extent parameter Φ is a value between 0 and 1. When Φ is equal to 0, species can be considered as totally segregated. While if Φ is equal to 1 complete mixing is accomplished.

3.2.2. Definition of reaction extent, η

For characterizing the reaction extent in the mixing zone, parameter η is expressed as

$$\eta = \frac{C_{B,phy} - C_{B,react}}{C_{B,phy}} \quad (5)$$

$C_{B,phy}$ and $C_{B,react}$ are the averaged concentration at the cross-sectional area of the mixing channel from the corresponding cases in the physical mixing experiments (i.e. experiment-II) and the reactive mixing experiments (i.e. experiment-III), respectively. Obviously, the value of η is also between 0 and 1. If η is equal to 0, $C_{B,phy}$ will be the same as $C_{B,react}$, which means no reaction occurs. Whereas, if η is equal to 1, the value of $C_{B,react}$ should be zero, which means reaction has consumed the species completely.

For clear comparison, three pairs of cases, i.e. Phy-2 and React-2, Phy-5 and React-5, and Phy-8 and React-8, are chosen. The Reynolds number in the mixing channel is the same, i.e. Re = 2000, while the relative momentum of jet flows is different. Figs. 6–8 show the mixing and reaction extent, i.e. the value of Φ and η, for each pair of corresponding cases at different positions along y direction in the measurement plane.

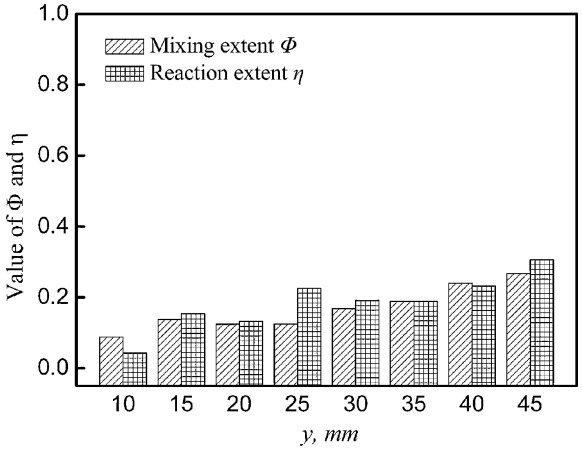

Fig. 6. Comparison of mixing and reaction extents for cases Phy-2 and React-2.

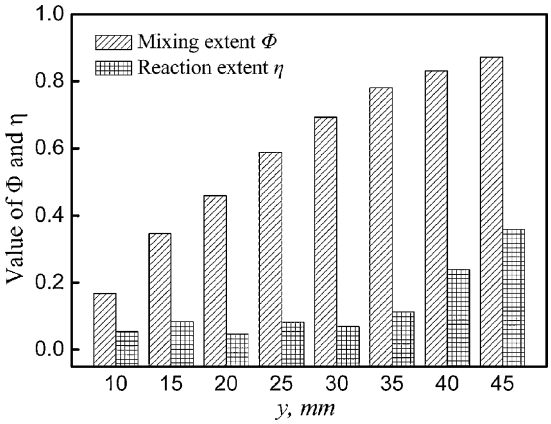

Fig. 7. Comparison of mixing and reaction extents for cases Phy-5 and React-5.

Three comparative relationships between mixing and reaction could be discovered from Figs. 6–8. In Fig. 6, i.e. the cases of Phy-2 and React-2, the relative momentum of jet flow is the lowest in these three pairs of cases. The values of Φ and η are similar along the y direction, and always maintain a low level around 0.1–0.3. Under this situation, mixing and reaction are both incomplete, and the rates of these two processes are both slow. Because the jet flow can hardly inject into the interior of bulk flow at a relative low momentum, species from liquid B can just transport into liquid A by turbulent and molecular diffusion, which causes a slow mixing rate. Thus, the reaction just takes place around the diffusion interface between the two streams, which leads to a low reaction extent.

In Fig. 7, another pattern is presented, where the value of Φ increases distinctly from 0.17 to 0.87 along y direction, which indicates that the mixing process could develop to a relatively complete status. However, the reaction extent parameter η is around the range of 0.1–0.2 in most regions of the mixing channel. When the y position is bigger than 40 mm, the value of η can merely rise to about 0.3. In these cases, mixing rate is obviously faster than that of reaction.

The comparative relationship in Fig. 8 is similar to Fig. 7, but the trend of reaction extent along the mixing channel has a few changes. From 0 to 25 mm in the y direction, the value of η maintains at 0, but it jumps to 0.15 abruptly, and increases gradually. This result reveals a fact, for these cases, that in the reactive mixing process, reaction does not occur until the mixing develops to a certain stage. Clearly, the mixing rate under this operating condition is faster than the reaction rate. Therefore we can de-couple the reactive mixing process into two isolated processes, i.e. firstly the mixing stage and secondly the reaction stage.

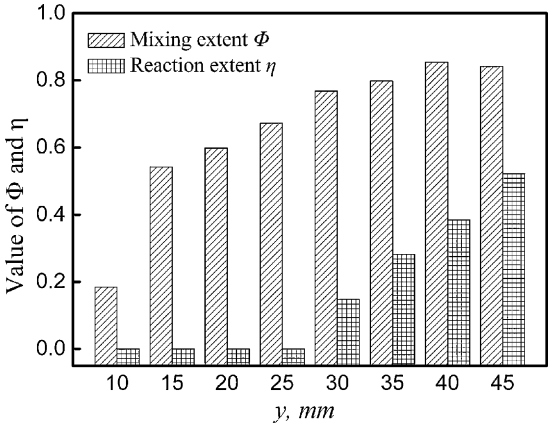

Fig. 8. Comparison of mixing and reaction extents for cases Phy-8 and React-8.

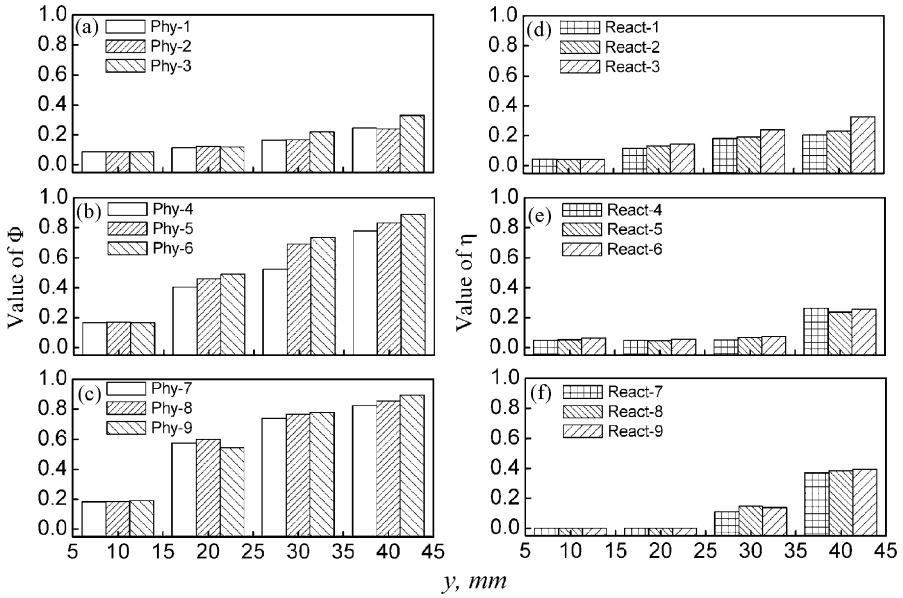

Fig. 9. Comparison of mixing and reaction extents for different Re numbers of mixing zone: (a) cases Phy-1, 2, 3; (b) cases Phy-4, 5, 6; (c) cases Phy-7, 8, 9; (d) cases React-1, 2, 3; (e) cases React-4, 5, 6; (f) cases React-7, 8, 9.

In order to demonstrate the effect of Re number in the mixing zones on the mixing and reaction processes, physical and reactive mixing processes are compared, respectively using the values of Φ and η in Fig. 9.

Fig. 9a–c express the variation of the (physical) mixing extent at different y positions with the change of Re number. To compare the results for identical jet flow momentum ratios, it can be observed that the Re number in the mixing zone has little effect on physical mixing extent. Especially, at small y values, the effect can be neglected. While with the flow development, the higher Re numbers may cause higher Φ values, i.e. higher mixing extent. For example in Fig. 9b, at the position of $y = 30$ mm, the increase of Re number from case Phy-4 to Phy-6, i.e. from 1300 to 2700, leads to an increase of Φ value from 0.523 to 0.735; and at the position of $y = 40$ mm, the rise of Φ is from 0.779 to 0.887.

Fig. 9d–f compare the reactive extent characterized by η under different Re numbers. Similar results can be observed that the reactive extent does not show clear dependence on the Re number under the same momentum ratios.

The results discussed above bring an insight that the relative rates of mixing and reaction in reactive mixing can be adjusted by the operating conditions. Intensified initial mixing by increasing the jet momentum of liquid B in these cases ensures that the mixing time scale is smaller than that of reactions, which results in the earlier accomplishment of the mixing process than the reactions. It is extremely important for some chemical production processes, such as the competing reactions, in which a certain excessive reagent in a local position would cause the generation of some by-products. Under these circumstances, if the mixing were finished before the reaction, the by-products would be prohibited to form since the reagents intend to react homogeneously in space in terms of the stoichiometrics of the material feeding ratio.

4. Conclusion

A new approach to implement the laser-induced fluorescence technique for reactive mixing measurement was advanced in this work. The novelty of the proposed reactive-LIF technique lay in the two aspects: (1) the inexpensive dye, i.e. Rhodamine-B, was used instead of very expensive dyes such as Rhodamine-2 or Rhodamine-WT; (2) the oxidation reaction mechanism (i.e. Fenton reaction) was employed to make the fluorescence signal from Rhodamine-B quenched so that the underlying reactive mixing process can be measured in time and in space.

This new reactive-LIF technique was tested by experiments in a mini-scale jet flow mixer. The purely physical mixing and the reactive mixing processes were investigated extensively by comparing the concentration fields under different operating conditions. The results showed that the mixing performance can be effectively influenced by the momentum ratio between jet and bulk flows. And the reactive mixing processes bear complex phenomenon in transient concentration fields. The coupled mixing and the reaction processes occurred simultaneously, unless the rapid mixing was achieved by tuning the operating conditions, and then the processes can be decoupled into two isolated ones.

Acknowledgements

Financial supports from National 973 Project of PR China (no. 2007CB714302), National Natural Science Foundation of China (NSFC) under the grant of no. 20776074 and a Foundation for the Author of National Excellent Doctoral Dissertation of PR China (no. 200245) are highly acknowledged.

References

[1] B.G. Lakatos, Population balance model for mixing in continuous flow systems, Chem. Eng. Sci. 63 (2008) 404–423.
[2] P.C. Chang, C.Y. Mou, D.J. Lee, Micromixing and macromixing effects in unsteady chemical reaction system, J. Phys. Chem. A 103 (1999) 5485–5489.
[3] L. Vicum, S. Ottiger, M. Mazzotti, L. Makowski, J. Baldyga, Multi-scale modeling of a reactive mixing process in a semibatch stirred tank, Chem. Eng. Sci. 59 (2004) 1767–1781.
[4] F. Schwertfirm, J. Gradl, H.C. Schwarzer, W. Peukert, M. Manhart, The low Reynolds number turbulent flow and mixing in a confined impinging jet reactor, Int. J. Heat Fluid Flow 28 (2007) 1429–1442.
[5] Y. Liu, H. Feng, M.G. Olsen, R.O. Fox, J.C. Hill, Turbulent mixing in a confined rectangular wake, Chem. Eng. Sci. 61 (2006) 6946–6962.
[6] R.O. Fox, On velocity-conditioned scalar mixing in homogeneous turbulence, Phys. Fluids 8 (1996) 2678–2691.
[7] D.L. Marchisio, R.O. Fox, A.A. Barresi, G. Baldi, On the comparison between presumed and full PDF methods for turbulent precipitation, Ind. Eng. Chem. Res. 40 (2001) 5132–5139.
[8] H. Feng, M.G. Olsen, Y. Liu, R.O. Fox, J.C. Hill, Investigation of turbulent mixing in a confined planar-jet reactor, AIChE J. 51 (2005) 2649–2664.
[9] R.O. Fox, V. Raman, A multienvironment conditional probability density function model for turbulent reacting flows, Phys. Fluids 16 (2004) 4551–4565.

[10] A. Gokarn, F. Battaglia, R.O. Fox, J.C. Hill, Simulations of mixing for a confined co-flowing planar jet, Comput. Fluids 35 (2006) 1228–1238.
[11] J. Baldyga, J.R. Bourne, Interaction between chemical reactions and mixing on various scales, Chem. Eng. Sci. 52 (1997) 457–466.
[12] J. Baldyga, J.R. Bourne, B. Zimmermann, Investigation of mixing in jet reactors using fast, competitive-consecutive reactions, Chem. Eng. Sci. 49 (1994) 1937–1946.
[13] J.R. Bourne, Mixing and the selectivity of chemical reactions, Org. Process Res. Dev. 7 (2003) 471–508.
[14] M.C. Fournier, L. Falk, J. Villermaux, A new parallel competing reaction system for assessing micromixing efficiency-experimental approach, Chem. Eng. Sci. 51 (1996) 5053–5064.
[15] A. Kölbl, M. Kraut, K. Schubert, The iodide iodate method to characterize microstructured mixing devices, AIChE J. 54 (2008) 639–645.
[16] P. Guichardon, L. Falk, Characterisation of micromixing efficiency by the iodide-iodate reaction system. Part I. Experimental procedure, Chem. Eng. Sci. 55 (2000) 4233–4243.
[17] G.G. Chen, G.S. Luo, S.W. Li, J.H. Xu, J. Wang, Experimental approaches for understanding mixing performance of a minireactor, AIChE J. 51 (2005) 2923–2929.
[18] S. Panic, S. Loebbecke, T. Tuercke, J. Antes, D. Boškovic, Experimental approaches to a better understanding of mixing performance of microfluidic devices, Chem. Eng. J. 101 (2004) 409–419.
[19] J.M. Rousseaux, L. Falk, H. Muhr, E. Plasari, Micromixing efficiency of a novel sliding-surface mixing device, AIChE J. 45 (1999) 2203–2213.
[20] J.R. Bourne, S. Yu, Investigation of micromixing in stirred tank reactors using parallel reactions, Ind. Eng. Chem. Res. 33 (1994) 41–55.
[21] I.L.M. Versehuren, J.G. Wijers, J.T.F. Keurentjes, Effect of mixing on product quality in semibatch stirred tank reactors, AIChE J. 47 (2001) 1731–1739.
[22] T.J. Johnson, D. Ross, L.E. Locascio, Rapid microfluidic mixing, Anal. Chem. 74 (2002) 45–51.
[23] T. Séon, J.P. Hulin, D. Salin, Laser-induced fluorescence measurement of buoyancy driven mixing in tilted tubes, Phys. Fluids 18 (2006) 041701.
[24] D.R. Unger, F.J. Muzzio, Laser-induced fluorescence technique for the quantification of mixing in impinging jets, AIChE J. 45 (1999) 2477–2486.
[25] M. Hoffmann, M. Schlüter, N. Räbiger, Experimental investigation of liquid–liquid mixing in T-shaped micro-mixers using μ-LIF and μ-PIV, Chem. Eng. Sci. 61 (2006) 2968–2976.
[26] A.W.K. Law, H. Wang, Measurement of mixing processes with combined digital particle image velocimetry and planar laser induced fluorescence, Exp. Therm. Fluid Sci. 22 (2000) 213–229.
[27] E. Hassel, S. Jahnke, N. Kornev, I. Tkatchenko, V. Zhdanov, Large-eddy simulation and laser diagnostic measurements of mixing in a coaxial jet mixer, Chem. Eng. Sci. 61 (2006) 2908–2912.
[28] P.C. Luo, Y. Cheng, Y. Jin, W.H. Yang, J.S. Ding, Fast liquid mixing by cross-flow impingement in millimeter channels, Chem. Eng. Sci. 62 (2007) 6178–6190.
[29] P.C. Luo, Y. Cheng, Y.Z. Zhao, Y. Jin, W.H. Yang, Millisecond mixing of liquid streams in a mixer model, Chem. Eng. Sci. 62 (2007) 5688–5695.
[30] P.C. Luo, Y. Cheng, Z.W. Wang, Y. Jin, W.H. Yang, Study on the mixing behavior of thin liquid-sheet impinging jets using the PLIF technique, Ind. Eng. Chem. Res. 45 (2006) 863–870.
[31] Y. Ito, S. Komori, A vibration technique for promoting liquid mixing and reaction in a microchannel, AIChE J. 52 (2006) 3011–3017.
[32] K. Shinohara, Y. Sugii, K. Okamoto, H. Madarame, A. Hibara, M. Tokeshi, T. Kitamori, Measurement of pH field of chemically reacting flow in microfluidic devices by laser-induced fluorescence, Meas. Sci. Technol. 15 (2004) 955–960.
[33] H.J.H. Fenton, Oxidation of tartaric acid in presence of iron, J. Chem. Soc. 65 (1894) 899–901.
[34] F. Haber, J.J. Weiss, The catalytic decomposition of hydrogen peroxide by iron salts, Proc. R. Soc. Lond., Ser. A 147 (1934) 332–345.
[35] W.G. Barb, J.H. Baxendale, P. George, K.R. Hargrave, Reactions of ferrous and ferric ions with hydrogen peroxide. Part I. The ferrous ion reaction, Trans. Faraday Soc. 47 (1951) 462–500.
[36] C. Walling, Fenton's reagent revisited, Accounts Chem. Res. 8 (1975) 125–131.
[37] S.H. Bossmann, E. Oliveros, S. Göb, S. Siegwart, E.P. Dahlen, L. Payawan, J.M. Straub, M. Wörner, A.M. Braun, New evidence against hydroxyl radicals as reactive intermediates in the thermal and photochemically enhanced Fenton reactions, J. Phys. Chem. A 102 (1998) 5542–5550.